VOL. 13, NO. 14, JULY 2018 ISSN 1819-6608
ARPN Journal of Engineering and Applied Sciences

www.arpnjournals.com

AN ANALYTICAL SOLUTION FOR THE DETERMINATION OF THE LOADS ACTING ON A SEMI-ELLIPTICAL WING: THE CASE OF THE REGGIANE RE 2005 WWII FIGHTER

Luca Piancastelli[1], Vincenzo Errani[1], Stefano Cassani[2], Federico Calzini[2] and Eugenio Pezzuti[3]
[1]Department of Industrial Engineering, Alma Mater Studiorum University of Bologna, Viale Risorgimento, Bologna, Italy
[2]MultiProjecta, Via Casola Canina, Imola, Italy
[3]Università di Roma "Tor Vergata", Dip. di Ingegneria dell'Impresa "Mario Lucertini", Via del Politecnico, Roma, Italy
E-Mail: luca.piancastelli@unibo.it

ABSTRACT

Many papers for the analytical solution of the lift distribution on a semi in semi-elliptical wing have been published. These works [1] usually approximate the solution by series expansion. This paper introduces an original method for the closed-form solution of this problem. The solution is possible through the use of symbolic manipulators. The wing of the WWII fighter "Reggiane Re 2005" has been solved analytically with the proposed method. The results are similar to the ones obtained by the panel-method and CFD. A CFD simulation of the Re 2005 at maximum speed demonstrates that these results are reasonable.

Keywords: lift, load, elliptical wing, analytical closed solution.

INTRODUCTION

The lift can be calculated with (1):

$$L = \frac{1}{2} \cdot \rho \cdot V^2 \cdot S \cdot Cl \quad (1)$$

The expression (1) is the resultant of a distributed load per unit length (half- wing) and, therefore, it is a function of the wing span. Cartesian reference system can be defined. The abscissa axis (x) coincides with the wing-root-chord and it is directed towards the trailing edge. The position of the origin is defined by the ordinate of the wing tip point. The ordinate axis (y) is directed towards the wingtip. The lift per unit length can be expressed as (2):

$$l(y) = \frac{1}{2} \cdot \rho \cdot V^2 \cdot c(y) \cdot cl(y) \quad (2)$$

The procedure that leads to the determination of the loads acting on the wing can be schematized as follows:

a) Determination of the function c(y);
b) Identify the function cl(y);
c) Definition the lift distribution per unit of length l(y);
d) Calculation of the expression T(y) (shear load function) as a function of y by integration of l(y);
e) Calculation of the expression the bending moment function M(y) by integration of the function T(y).

Determination of the function C(y) that describes the wing-chord-length with span y

From the analysis of the original drawings it is possible to define the function that describes the chord length with the distance from the root (y-axis). For the trailing edge of an elliptical equation (3) can be used:

$$x(y) = -\sqrt{a^2 \cdot (1 - \frac{y^2}{b^2})} \quad (3)$$

Where the semi-axis are a=1.619m and b=5.5 m. For the leading edge, equation (4) holds in the interval {0<y<4.742m}:

$$x_{i1}(y) = -0.0562y + 0.7465 \quad (4)$$

Equation (4) describes a line that terminates in the point $P_{tipfillet}$ that has the following coordinates: {0.480, 4.742}. From this point on, another curve to describe the fillet tip should be used. For the leading edge of the tip, the "elliptical" function (5) holds in the interval {4.742 <y <5.5m}:

$$x_{i2}(y) = -\sqrt{a_2^2 \cdot (1 - \frac{(y-h)^2}{b_2^2})} \quad (5)$$

Where the ellipse axis and the y-value of the ellipse-centre h are calculated by imposing the following conditions:

c1) The line of the equation (4) is tangent to the ellipse (5) at the end point $P_{tipfillet}$ {0.480, 4.742}.
c2) The centre of the ellipse is on the y axis. The coordinate of the centre of the ellipse (5) will then be {h, 0}.
c3) The wing tip point P_{tip} {0, 5. 5} belongs to (5).

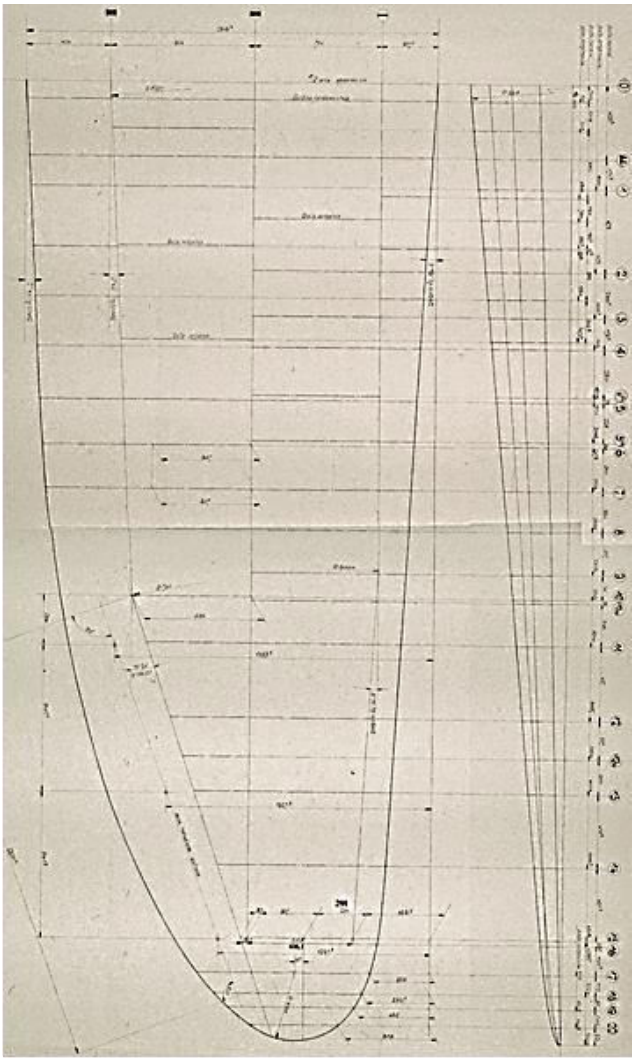

Figure-1. Original drawing of the Re2005 wing.

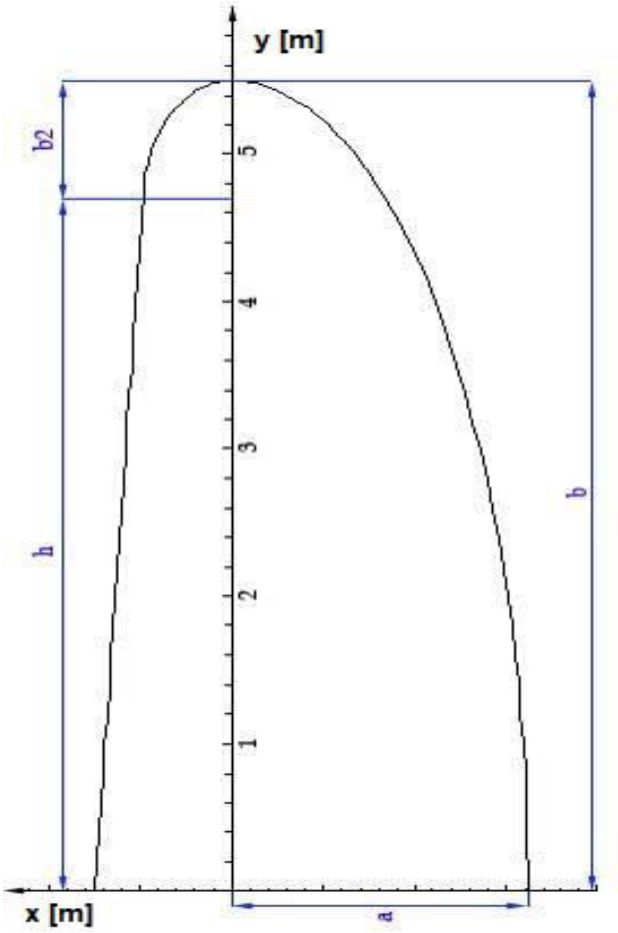

Figure-2. Re 2005 wing planform from (3) (4) (5).

The values of {a2=b2=0.482, h=4.66} can be obtained from the above conditions ***c1***, ***c2*** and ***c3***.

It is then possible to draw the wing planform (Figure-2):

As it can be seen from Figure-3 the functions (3) (4) and (5) approximate very well the true plan form of the Re 2005 wing (see also Figures 1 and 3).

The chord functions (5) (6) can then be calculated from (2) (3) and (4):

$$Cl(y) = x_{t1}(y) - x(y) = -0.0562y + 0.7465 + \sqrt{(1.619)^2 \cdot (1 - \frac{y^2}{(5.5)^2})} \quad (6)$$

Equation (6) holds for 0 <y <4.742m.

$$C2(y) = x_{t2}(y) - x(y) = -\sqrt{(0.482)^2 \cdot (1 - \frac{(y-4.660)^2}{(0.839)^2})} + \sqrt{(1.619)^2 \cdot (1 - \frac{y^2}{(5.5)^2})} \quad (7)$$

Equation (7) holds for 4.742 <y <5.5m.

Identification of the function cl(y) that describes the evolution of the linear lift coefficient with y

The study of original drawings of the Re 2005 has led to the following conclusions:

a) the airfoils evolve from a root similar to a NACA 0016, to an end corresponding to a NACA 23009;

b) the wing of the aircraft has a positive "riggers' angle of incidence" of 3 degrees (this means that the root chord is rotated clockwise of 3 degrees from the propeller-axis, on the sidewiew with the propeller on the left side).

c) The wing is twisted. Twist decreases the local chord's incidence from root to tip (washout).

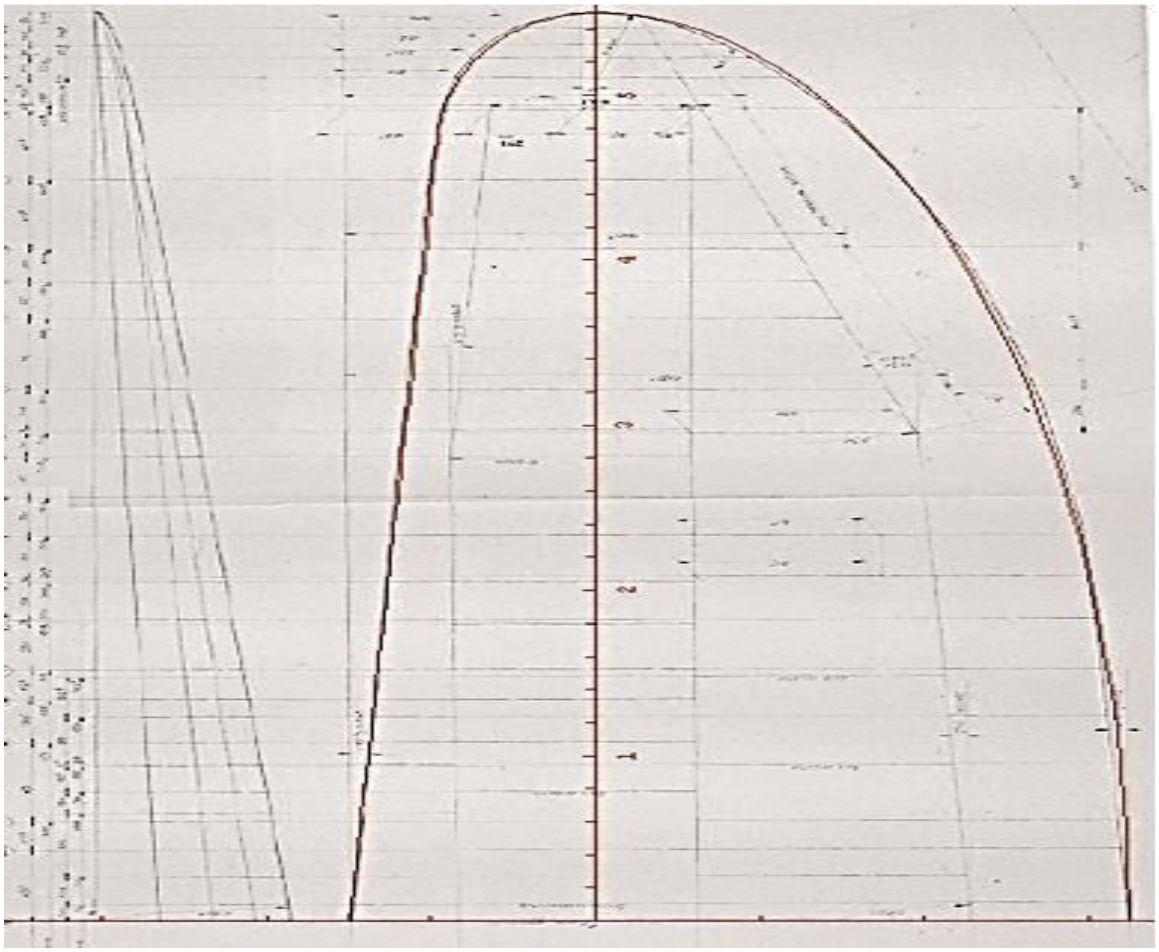

Figure-3. Calculated planform (red) of Figure-2 superimposed on the original Reggiane drawing.

To determine the $C_l(y)$ only 14 of 34 airfoils of the original drawings were considered. Each of them was imported into the software Java Foil [2] with its pitch angle, in order to determine the C_l value. The values are calculated at the Reynolds number corresponding to following leveled flying condition: 175m/s@7,200m ISA+0°C [3-29]. The results are summarized in Table-1.

Table-1. Javafoil results

# on drawings	**Chord** (m)	**y** (m)	**Riggers' angle of incidence**(degrees)	**Cl**
0	2.3655	0	3.00	0.371
1	2.2841	0.78	2.66	0.247
3	2.2261	1.355	2.38	0.236
5	2.1735	1.82	2.12	0.225
7	2.114	2.328	1.83	0.21
9	2.02	2.805	1.57	0.21
11	1.9264	3.21	1.33	0.2
12	1.802	3.637	1.01	0.183
13	1.642	4.064	0.64	0.177
14	1.456	4.405	0.32	0.158
15	1.1905	4.905	-0.03	0.104
17	1.01	5.105	-0.17	0.09

19	0.743	5.305	-0.31	0.07
20	0.531	5.44	-0.43	0.05
Tip	0	5.5		0

Figure-4 shows that the JavaFoil results. An elliptic function described well the results of JavaFoil (see Figure-4). Therefore, for simplicity, an elliptic function is adopted for the *cl(y)* (8):

$$cl(y) = 0.249\sqrt{(1-\frac{y^2}{5.5^2})} \quad (8)$$

This assumption makes it possible to evaluate the average value of Cl for the wing (9).

$$Cl_{mean} = \frac{\int_0^{l_{wing}} 0.249\sqrt{(1-\frac{y^2}{5.5^2})}dy}{l_{wing}\times 2} = 0.196 \quad (9)$$

Definition of the lift distribution per unit of length l(y)

Function (9) can be obtained by combining the equations (2), (6) and (8). This function holds in the interval y ϵ {0, 4. 742}.

$$l1(y) = \frac{1}{2}\rho C1(y)Cl(y)V^2 = 2202.191\sqrt{1-0.033y^2}(0.746-0.056y+1.619\sqrt{1-0.033y^2} \quad (10)$$

Function (11) holds in the interval: yϵ{4.742,5.5}.

$$l2(y) = \frac{1}{2}\rho C2(y)Cl(y)V^2 = 3565.347-117.862y^2+229.949\sqrt{(y-5.5)^2(y-2.82)(y+5.5)} \quad (11)$$

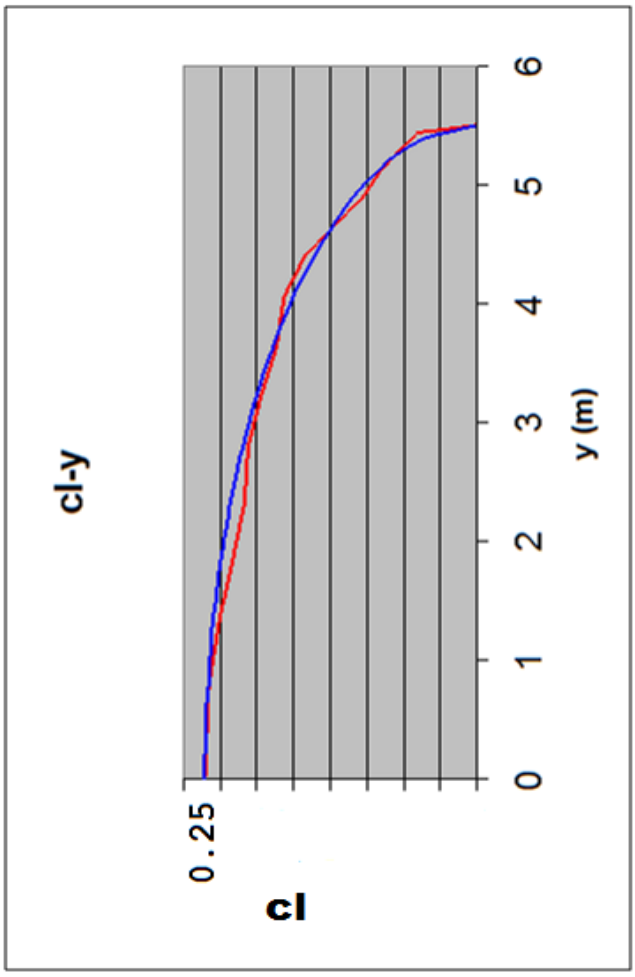

Figure-4. Calculated planform (red) of Figure-2 superimposed on the original Reggiane drawing.

The results are shown in Figure-5.

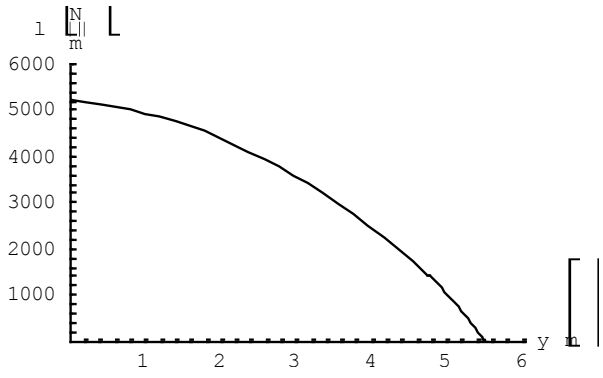

Figure-5. Cl(y) from equations (9) and (10).

The reliability of the results can be verified by calculating the total lift L (11).

$$L = 2\int_{0}^{4.742} l1(y)dy + \int_{4.742}^{5.5} l2(y)dy = 37785N \quad (12)$$

An acceptable value of weight for Re 2005 is 35400N. The value calculated by (11) is then overestimated. This is logical since the fuselage and the propeller reduces the overall efficiency of the wing.

The shear load function T(y)

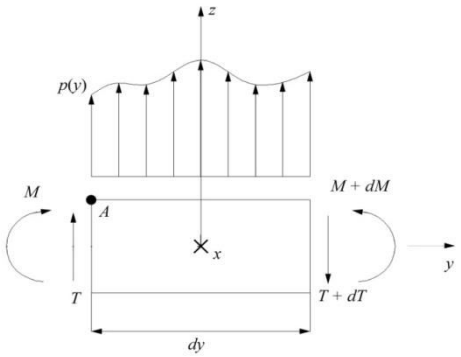

Figure-6. Bending M and shear T.

From Figure-6, it is possible to see that static equilibrium equations (13) (14) can be used to for the shear load function.

$$dT = p\,dy \quad (13)$$

$$dM = T\,dy \quad (14)$$

T(y) (14) (15) can then be calculated with (13) and (14) from the distributed load of equations (9) and (10). The function (14) holds for 0 <y <4.742m.

$$T2(y) = \int_{0}^{y} l2(y)dy + A2 = A2 + 3565.347y - 29.287y^3 + \frac{\sqrt{(y-5.5)^2(y-3.82)(y+5.5)}}{(y-5.5)\sqrt{(y-3.82)(y+5.5)}} + \frac{1}{(y-5.5)\sqrt{(y-3.82)(y+5.5)}}(1.8396\sqrt{233+25(y-3.82)} - 1.583(y-3.82)^{\frac{3}{2}} + 8.333(y-3.82)^{\frac{5}{2}} \times \sqrt{(y-5.5)^2(y-3.82)(y+5.5)} + \frac{31658\sqrt{(y-5.5)^2(y-3.82)(y+5.5)}\,ASinh(0.327\sqrt{(y-3.82)})}{(y-5.5)\sqrt{(y-3.82)(y+5.5)}} \quad (15)$$

While the function (15) can be used for 4.742 <y<5.5m.

$$T1(y) = \int_{0}^{y} l1(y)dy + A1 = A1 + 2202.9(1.619y - 0.017y^3 - 0.018(y-21.347)(y+1.412)\sqrt{1-033y^2} + 2.052ASinh(0.181y)) \quad (16)$$

The integration constants A1 and A2 can be found by the imposition of the following boundary conditions:

- Null shear load at tip: $T2_{(Y=5.5)}$=0. From which it is possible to calculate A2=-13783.6.
- From the continuity of the shear at y=4.742m. $T2_{(y=4.742)}$=$T1_{(y=4.742)}$, it is possible to calculate A1=-20140.9.

It is then possible to calculate the design shear load for the wing. In this calculation a load factor of 8 and a safety factor of 1.5 were included. The results are shown in Figure-7.

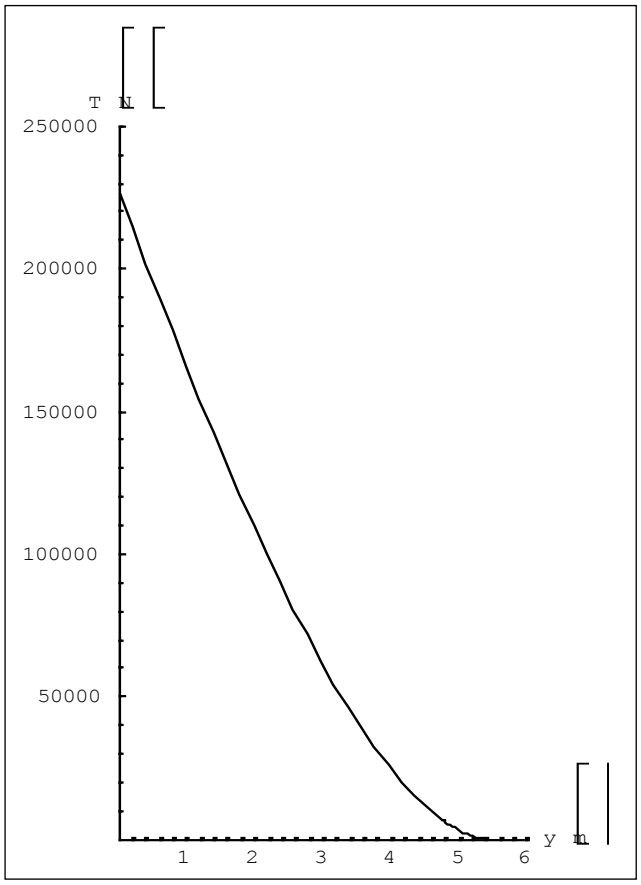

Figure-7. Shear load T along the wing (y_{root}=0, y_{tip}=5.5) from equations (9) and (10) The bending moment M(y).

The integration of T(y) (14) (15) makes it possible to calculate M(y) (16) (17).

$$M2(y) = \int_{0}^{y} T2(y)dy + B2 = (B2 + 13793.579y + 1782.673y^2 - 9.821y^3 + \frac{\sqrt{(y-5.5)^2(y-3.82)(y+5.5)}}{(y-5.5)\sqrt{(y-3.82)(y+5.5)}} + \frac{y\sqrt{(y-5.5)^2(y-3.82)(y+5.5)}}{(y-5.5)\sqrt{(y-3.82)(y+5.5)}} - \frac{48325.067\sqrt{(0.590+0.107y)(y-5.5)^2(y-3.82)^2(y+5.5)}}{\sqrt{(y-5.5)^2(y-3.82)(y+5.5)}} \frac{1}{(y-5.5)\sqrt{(y-3.82)(y+5.5)}}(3.832(y-14.230)(y-2.403)\times \sqrt{(y-5.5)^2(y-3.82)(y+5.5)}(6.473+y)\sqrt{137.5+25y}) + \frac{174639.251(y-5.5)\sqrt{(y-3.82)(y+5.5)}A\sinh(0.327\sqrt{y-3.82})}{\sqrt{(y-5.5)^2(y-3.82)(y+5.5)}} + \frac{31658.804(y-5.5)(y-3.82)^{\frac{3}{2}}(y+5.5)^{\frac{1}{2}}A\sinh(0.327\sqrt{y-3.82})}{\sqrt{(y-5.5)^2(y-3.82)(y+5.5)}}) \quad (17)$$

Equation 17 holds for for 0<y<4.742 m. While equation (18) holds for for 4.742<y<5.5m.

$$M1(y) = \int_0^y T1(y)dy + B1 = B1 - 22014.894y + 1782.673y^2 - 9.821y^4 y + 24864.526\sqrt{1-033y^2} + 2202.191\sqrt{1-033y^2}(-3.763 + 0.354y + 0.124y^2 - 0.004y^3) + 2573.886ASinh(0.181y) + 4520.820ASinh(0.181y) \quad (18)$$

The integration constants B1 and B2 can be found through the imposition of the following boundary conditions:

- zero bending moment at the tip: $M2_{(Y=5.5)}=0 \rightarrow B2=30194.7$;
- Continuity of the bending moment at Y=4.742m. $M2_{(Y=4.742)}=M1_{(Y=4.742)} \rightarrow B1=22744.2$.

CONCLUSIONS

The use of modern software makes it possible to calculate the closed form solution of the lift, the shear and the bending moment for a semi-elliptical wing. The example of the Reggiane Re 2005 WWII fighter is shown in this paper as an example.

REFERENCES

[1] M. Munk. 1922. The twisted wing with elliptic plan form. NACA Technical Note No. 109.

[2] http://www.mh-aerotools.de/airfoils/javafoil.htm. Accessed 2018-04-16.

[3] L. Piancastelli, L. Frizziero, S. Marcoppido, E. Pezzuti. 2012. Methodology to evaluate aircraft piston engine durability. edizioni ETS. International Journal of Heat & Technology. ISSN 0392-8764, 30(1): 89-92, Bologna.

[4] L. Piancastelli, L. Frizziero, G. Donnici. 2015. The Meredith ramjet: An efficient way to recover the heat wasted in piston engine cooling. Asian Research Publishing Network (ARPN). Journal of Engineering and Applied Sciences. ISSN 1819-6608, 10(12): 5327-5333, EBSCO Publishing, 10 Estes Street, P.O. Box 682, Ipswich, MA 01938, USA.

[5] L. Piancastelli, A. Gatti, L. Frizziero, L. Ragazzi, M. Cremonini. 2015. CFD analysis of the Zimmerman's V173 stol aircraft. Asian Research Publishing Network (ARPN). Journal of Engineering and Applied Sciences. ISSN 1819-6608, 10(18): 8063-8070, EBSCO Publishing, 10 Estes Street, P.O. Box 682, Ipswich, MA 01938, USA.

[6] L. Piancastelli, L. Frizziero. 2014. Turbocharging and turbo compounding optimization in automotive racing. Asian Research Publishing Network (ARPN). Journal of Engineering and Applied Sciences. ISSN 1819-6608, 9(11): 2192-2199, EBSCO Publishing, 10 Estes Street, P.O. Box 682, Ipswich, MA 01938, USA

[7] L. Piancastelli, L. Frizziero, G. Donnici. 2014. The common-rail fuel injection technique in turbocharged di-diesel-engines for aircraft applications. Asian Research Publishing Network (ARPN). Journal of Engineering and Applied Sciences. ISSN 1819-6608, 9(12): 2493-2499, EBSCO Publishing, 10 Estes Street, P.O. Box 682, Ipswich, MA 01938, USA

[8] L. Piancastelli, L. Frizziero, G. Donnici. 2015. Turbomatching of small aircraft diesel common rail engines derived from the automotive field. Asian Research Publishing Network (ARPN). Journal of Engineering and Applied Sciences. ISSN 1819-6608, 10(1): 172-178, EBSCO Publishing, 10 Estes Street, P.O. Box 682, Ipswich, MA 01938, USA

[9] L. Piancastelli, L. Frizziero. 2015. Supercharging systems in small aircraft diesel common rail engines derived from the automotive field. Asian Research Publishing Network (ARPN), "Journal of Engineering and Applied Sciences. ISSN 1819-6608, 10(1): 20-26, EBSCO Publishing, 10 Estes Street, P.O. Box 682, Ipswich, MA 01938, USA.

[10] P.P. Valentini, E. Pezzuti E. Computer-aided tolerance allocation of compliant ortho-planar spring mechanism. Int. Jou. Of computer applications in technology. 53: 369-374, ISSN: 0952-8091, doi: 10.1504/IJCAT.2016.076801.

[11] E. Pezzuti, PP. Valentini PP. Accuracy in fingertip tracking using Leap Motion Controller for interactive virtual applications. Int. Jour. On interactive design and manufacturing, pp. 1-10, ISSN: 1955-2513, doi: 10.1007/s12008-016-0339-y

[12] E.Pezzuti E, PP. Valentini P. Design and interactive simulation of cross-axis compliant pivot using dynamic spline. Int. Jour. On interactive design and manufacturing. 7: 261-269, ISSN: 1955-2513, doi: 10.1007/s12008-012-0180-x

[13] L. Piancastelli, S. Cassani. 2017. Maximum peak pressure evaluation of an automotive common rail diesel piston engine head. Asian Research Publishing Network (ARPN). Journal of Engineering and Applied Sciences. ISSN 1819-6608, 12(1): 212-218, EBSCO Publishing, 10 Estes Street, P.O. Box 682, Ipswich, MA 01938, USA.

[14] S. Cassani. 2017. Airplane design: the superiority of fsw aluminum-alloy pure monocoque over cfrp black constructions. Asian Research Publishing Network (ARPN). Journal of Engineering and Applied Sciences. ISSN 1819-6608, 12(2): 377-361, EBSCO Publishing, 10 Estes Street, P.O. Box 682, Ipswich, MA 01938, USA.

[15] L. Piancastelli, S. Cassani. 2017. Power speed reduction units for general aviation part 2: general design, optimum bearing selection for propeller driven aircrafts with piston engines. Asian Research Publishing Network (ARPN). Journal of Engineering and Applied Sciences. ISSN 1819-6608, 12(2): 544-550, EBSCO Publishing, 10 Estes Street, P.O. Box 682, Ipswich, MA 01938, USA.

[16] L. Piancastelli, S. Cassani. 2017. Power speed reduction units for general aviation part 5: housing/casing optimized design for propeller-driven aircrafts and helicopters. Asian Research Publishing Network (ARPN). Journal of Engineering and Applied Sciences. ISSN 1819-6608, 12(2): 602-608, EBSCO Publishing, 10 Estes Street, P.O. Box 682, Ipswich, MA 01938, USA.

[17] L. Piancastelli, S. Cassani. 2017. power speed reduction units for general aviation part 3: simplified gear design piston-powered, propeller-driven general aviation aircrafts. Asian Research Publishing Network (ARPN). Journal of Engineering and Applied Sciences. ISSN 1819-6608, 12(3): 870-874, EBSCO Publishing, 10 Estes Street, P.O. Box 682, Ipswich, MA 01938, USA.

[18] L. Piancastelli, S. Cassani. 2017. Power Speed Reduction Units For General Aviation Part 4: Simplified Gear Design For Piston-Powered, Propeller-Driven Heavy Duty Aircrafts And Helicopters. Journal of Engineering and Applied Sciences. ISSN 1819-6608, 12(5): 1533-1539, EBSCO Publishing, 10 Estes Street, P.O. Box 682, Ipswich, MA 01938, USA.

[19] L. Piancastelli, S. Migliano, S. Cassani. 2017. An extremely compact, high torque continuously variable power transmission for large hybrid terrain vehicles. Journal of Engineering and Applied Sciences. ISSN 1819-6608, 12(6): 1796-1800, EBSCO Publishing, 10 Estes Street, P.O. Box 682, Ipswich, MA 01938, USA.

[20] L. Piancastelli, S. Cassani. 2017. Mapping Optimization For Partial Loads Of Common Rail Diesel Piston Engines. Journal of Engineering and Applied Sciences. ISSN 1819-6608, 12(7): 2223-2229, EBSCO Publishing, 10 Estes Street, P.O. Box 682, Ipswich, MA 01938, USA.

[21] L. Piancastelli, S. Cassani. 2017. High Altitude Operations With Piston Engines Power Plant Design Optimization Part V: Nozzle Design And Ramjet General Considerations. Journal of Engineering and Applied Sciences. ISSN 1819-6608, 12(7): 2242-2247, EBSCO Publishing, 10 Estes Street, P.O. Box 682, Ipswich, MA 01938, USA.

[22] L. Piancastelli, R. V. Clarke, S. Cassani. 2017. Diffuser Augmented Run The River And Tidal Picohydropower Generation System. Journal of Engineering and Applied Sciences. ISSN 1819-6608, 12(8): 2678-2688, EBSCO Publishing, 10 Estes Street, P.O. Box 682, Ipswich, MA 01938, USA.

[23] L. Piancastelli, M. Gardella, S. Cassani. 2017. Cooling System Optimization For Light Diesel Helicopters. Journal of Engineering and Applied Sciences. ISSN 1819-6608, 12(9): 2803-2808, EBSCO Publishing, 10 Estes Street, P.O. Box 682, Ipswich, MA 01938, USA.

[24] L. Piancastelli, S. Cassani. 2017. Study And Optimization Of A Contra-Rotating propeller hub for convertiplanes. part 1: vto and hovering. journal of Engineering and Applied Sciences. ISSN 1819-6608, 12(11): 3451-3457, EBSCO Publishing, 10 Estes Street, P.O. Box 682, Ipswich, MA 01938, USA.

[25] L. Piancastelli, S. Cassani. 2017. On The Conversion Of Automotive Engines For General Aviation. Journal of Engineering and Applied Sciences. ISSN 1819-6608, 12(13): 4196-4203, EBSCO Publishing, 10 Estes Street, P.O. Box 682, Ipswich, MA 01938, USA.

[26] L. Piancastelli, S. Cassani. 2017. convertiplane cruise performance with contra-rotating propeller. Journal of Engineering and Applied Sciences. ISSN 1819-6608, 12(19): 5554-5559, EBSCO Publishing, 10 Estes Street, P.O. Box 682, Ipswich, MA 01938, USA.

[27] L. Piancastelli, S. Cassani. 2017. Tribological Problem Solving In Medium Heavy Duty Marine Diesel Engine Part 1: Journal Bearings. Journal of Engineering and Applied Sciences. ISSN 1819-6608,

12(22): 6533-6541, EBSCO Publishing, 10 Estes Street, P.O. Box 682, Ipswich, MA 01938, USA.

[28] A. Ceruti, T. Bombardi, T., L. Piancastelli. 2016. Visual Flight Rules Pilots Into Instrumental Meteorological Conditions: a Proposal for a Mobile Application to Increase In-flight Survivability. International Review of Aerospace Engineering (IREASE). 9(5).

[29] L. Piancastelli, A. Burnelli A., S. Cassani. 2017. Validation of a simplified method for the evaluation of pressure and temperature on a RR Merlin XX head, International Journal of Heat and Technology. 35(1): 549558. DOI: 10.18280/ijht.350311.

SYMBOLS

Symbol	Description	Unit	Value
L	Lift	N	
V	Speed	m/s	175
S	Wing area	m^2	
Cl	Lift coefficient	-	
ρ	Air density	kg/m^3	
l(y)	Lift function along the wing span (y axis)	N/m	
c(y)	Cord length function along y	m	
Cl(y)	Lift coefficient function along y	-	
x(y)	Trailing edge function	m	
a	Semi-minor axis of x(y)	m	1.619
b	Semi-minor axis of x(y)	m	5.5
$x_{i1}(y)$	Leading edge function (linear part)	m	
$x_{i2}(y)$	Leading edge function (fillet tip)	m	
a_2	Semi-minor axis of $x_{i1}(y)$	m	0.482
b_2	Semi-minor axis of $x_{i1}(y)$	m	0.482
h	Coordinate y of the center of the Ellipse $x_{i2}(y)$	m	4.66
C1(y)	Cord length function along y. yϵ[0. 4.742]	m	
C2(y)	Cord length function along y. yϵ[4.742. 5.5]		
l_{wing}	Wingspan/2	m	5.5
Cl(y)	Lift coefficient function along y		
Cl_{mean}	Average wing lift coefficient		
l1(y)	Lift function along y. yϵ[0. 4.742]	N	
l2(y)	Lift function along y. yϵ[4.742. 5.5]	N	
T1(y)	Shear load function along y. yϵ[0. 4.742]	N	
T2(y)	Shear load function along y. yϵ[4.742. 5.5]	N	
M1(y)	Bending moment function along y. yϵ[0. 4.742]	Nm	
M2(y)	Bending moment function along y. yϵ[4.742. 5.5]	Nm	